

# Selective and enantioselective analysis of mono- and disaccharides using surface plasmon resonance spectroscopy and imprinted boronic acid-functionalized Au nanoparticle composites

Yaniv Ben-Amram, Michael Riskin and Itamar Willner\*

Received 26th April 2010, Accepted 14th July 2010

DOI: 10.1039/c0an00268b

A method was developed for the synthesis of molecularly imprinted Au nanoparticle (NP) composites on electrodes by electrochemical means. The resulting composites include specific recognition sites for mono- or disaccharides. The method is based on the formation of a boronate complex between the respective saccharide and the boronic acid ligands associated with the Au NPs. The electropolymerization of the Au NPs leads, after cleavage of the respective boronate esters, and removal of the saccharide, to specific recognition sites for the association of the imprinted monosaccharides or disaccharides. The binding of the saccharides to the imprinted sites is followed by surface plasmon spectroscopy (SPR). The changes in the refractive index of the Au NP composites upon the binding of the saccharides to the imprinted sites are amplified by the coupling between the localized plasmon associated with the NPs and the surface plasmon wave propagating on the Au surface. This leads to the highly sensitive stereoselective and chiroselective detection of monosaccharides and disaccharides.

## Introduction

Molecularly imprinted organic or inorganic polymers have attracted substantial research efforts<sup>1,2</sup> and have been extensively used in chromatographic separation,<sup>3</sup> slow release systems,<sup>4</sup> catalytic materials,<sup>5</sup> and as sensing matrices.<sup>6</sup> There are, however, several limitations of the application of molecularly imprinted polymers for sensing purposes. As the number of imprinted sites is limited, the sensitivity of the sensors is quite low, and relatively thick sensing matrices are required. Also, the fact that the sensing interfaces are relatively thick means that it is difficult to transduce the sensing events, resulting in relatively long response times. Several physical methods, for example, electrochemical,<sup>7</sup> field-effect-transistors,<sup>8</sup> piezoelectric,<sup>9</sup> or competitive fluorescence methods,<sup>10</sup> have been implemented to transduce the sensing events in molecularly imprinted polymers. Indeed, selective<sup>11</sup> and chiroselective<sup>12</sup> sensing platforms with imprinted polymers have been reported.

Metallic nanoparticles (NPs) provide high surface area elements with unique optical<sup>13</sup> and catalytic<sup>14</sup> properties. For example, metallic NPs, such as Au or Ag NPs, exhibit size-controlled localized plasmon excitons.<sup>15</sup>

Also, numerous synthetic methods used to prepare metal NPs of controlled dimensions and shapes, and various methods used to modify the NPs with chemical functionalities, such as monolayers or polymers, turn the NPs into useful sensing elements.<sup>16</sup> Indeed, numerous optical<sup>17</sup> or electrochemical<sup>18</sup> sensors based on metallic NPs have been reported over the last two decades.

Surface plasmon resonance (SPR) is a versatile method that can be used to probe refractive index changes that occur on metal

surfaces, such as gold or silver, as a result of chemical sensing events.<sup>19</sup> This technique has been widely applied in the development of sensors and biosensors.<sup>20</sup> The sensitivity of the SPR sensors is, however, limited by the refractive index changes induced upon the binding of the analytes to the sensing matrices, and the resulting measurable shifts in the SPR spectra. While the association of macromolecules, such as proteins, to the sensing matrices stimulates a high refractive change even at low loading, low-molecular-weight substrates at low coverage yield minute refractive index changes that eliminate their detection by SPR. Amplified SPR sensing has been achieved by the conjugation of latex particles,<sup>21</sup> liposomes,<sup>22</sup> or proteins<sup>23</sup> to the recognition complexes. Specifically, metallic nanoparticles, such as Au or Ag, were used as labels for amplified SPR sensing. The coupling between the localized plasmon of the NPs and the surface plasmon wave associated with the thin metal film, acting as the sensing support, was found to shift the SPR energy, and thus enhance the SPR spectral shifts.<sup>24</sup> Indeed, numerous studies have reported on the use of metal NP conjugates as amplifying labels for sensing events, such as the analysis of antigen-antibody complexes,<sup>25</sup> DNA hybridization,<sup>26</sup> or the probing of biocatalytic transformations.<sup>27</sup> In a series of recent studies we reported on the electrochemical polymerization of thioaniline-functionalized Au NP composites on Au surfaces and on the molecular imprinting of specific recognition sites in the aggregated Au NPs. The three-dimensional conductivity of the metallic NP composites, and the coupling of the localized plasmon of the Au NPs with the Au surface enabled the electrochemical or SPR selective and chiroselective detection of the analytes that bind to the imprinted sites. For example, molecularly imprinted Au NP matrices have been used for the electrochemical<sup>28</sup> or SPR<sup>29</sup> detection of trinitrotoluene (TNT). Similarly, imprinted Au NP matrices have been used for the ultrasensitive SPR detection of the 1,3,5-trinitrotriazine (RDX) explosive.<sup>30</sup> Also, the co-immobilization of

Institute of Chemistry, The Hebrew University of Jerusalem, Jerusalem, 91904, Israel. E-mail: willnea@vms.huji.ac.il; Fax: +972-2-6527715; Tel: +972-2-6585272

specific ligands, and the electropolymerizable thioaniline units on the Au NPs enabled the binding of the analytes to the ligands, and the generation of specific imprinted recognition sites for the analyte in the electropolymerized Au NP composites. For example, the electropolymerization of Au NPs modified with a mixed monolayer of cysteine/thioaniline in the presence of different amino acids led to imprinted Au NP matrices that revealed selective and chiroselective sensing toward different amino acids.<sup>31</sup>

The boronic acid ligand binds to vicinal diols and forms the respective boronate esters.<sup>32</sup> Different sensor platforms, based on the boronic acid ligand, for the detection of saccharides<sup>33</sup> or neurotransmitters<sup>34</sup> have been reported. Also, polymerizable monomers, containing the boronic acid ligand, have been used to synthesize imprinted polymer matrices for different saccharides.<sup>35</sup> Similarly, Au NPs modified with a mixed monolayer of thioaniline/mercaptophenyl boronic acid have been used for the electrochemical synthesis of imprinted Au NP matrices for a series of vicinal-diol-containing antibiotics.<sup>36</sup> Selective analysis of the different antibiotics using SPR as readout signal was demonstrated in these systems. Here we report on the electrochemical synthesis of imprinted selective and chiroselective Au NP composites for the sensing of monosaccharides and disaccharides. We compare the effectiveness of sensing of the different analytes by the imprinted and non-imprinted composites, and we highlight the influence of the imprinting process on the sensitivities and the selectivities of the sensing matrices.

## Experimental

### Synthesis of the functionalized Au nanoparticles

Au nanoparticles functionalized with 4-mercaptoaniline, (1), mercaptoethane sulfonic acid, (2), and mercaptophenyl boronic acid, (3), were prepared by mixing 197 mg Au(III) chloride hydrate, HAuCl<sub>4</sub>, in 10 ml methanol solution with a 5 ml methanol solution that included 9 mg of 3, 35 mg of 2 and 7 mg of 1. The two solutions were stirred in the presence of 2.5 ml glacial acetic acid in an ice bath for 1 h. Subsequently, 7.5 ml of 1 M sodium borohydride, NaBH<sub>4</sub>, aqueous solution, was added dropwise, resulting in a dark colored solution associated with the presence of the Au NPs. The solution was stirred for fourteen hours in an ice bath. The particles were successively washed and centrifuged (twice in each solvent) with methanol, ethanol and diethyl ether. A mean particle size of *ca.* 4.5 ± 0.5 nm was estimated using TEM measurements.

### Chemical modification of the electrode surface

4-Aminothiophenol-functionalized electrodes were prepared by immersing Au slides for 48 h in a 10 mM 4-aminothiophenol ethanolic solution. The functionalized Au NPs, 2 mg ml<sup>-1</sup>, were dissolved in a 50 mM HEPES buffer solution (pH = 9.2) and electropolymerized on the 4-aminothiophenol-modified Au electrode. Electropolymerization was performed by applying 10 potential cycles between -0.25 V and 0.7 V vs. a Ag wire quasi-reference electrode (QRE) followed by the application of a constant potential, *E* = 0.7V vs. a Ag QRE, for 2 h. The resulting films were then washed with the background HEPES buffer solution to exclude any residual monomer from the

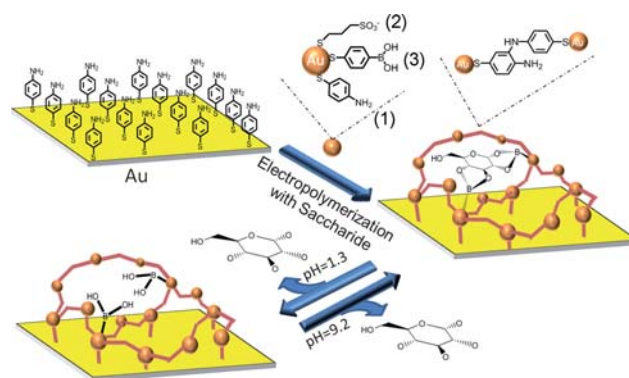
electrode. Similarly, saccharide-imprinted bis-aniline-crosslinked films were prepared using a mixture containing 0.5 M of the selected saccharide with 2 mg ml<sup>-1</sup> of the functionalized Au NPs. Extraction of the saccharide from the film was carried out by immersing the electrodes in a 0.1 M H<sub>2</sub>SO<sub>4</sub> solution, pH = 1.3, for 15 min. Subsequently, the film was washed thoroughly using HEPES buffer (pH = 9.2). Removal of the saccharide from the electropolymerized film was verified by obtaining a steady SPR curve resembling the SPR spectrum of the non-imprinted Au NP composite.

### Instrumentation and measurements

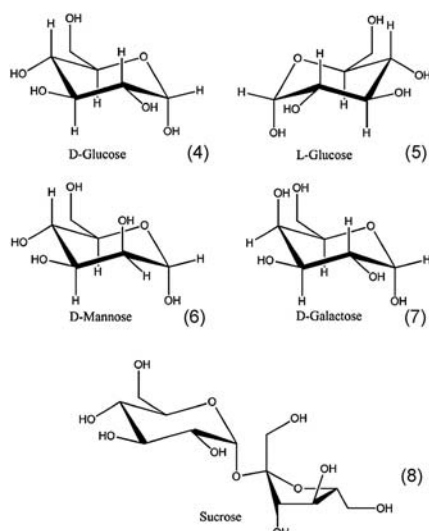
An SPR Kretschmann type spectrometer NanoSPR 321 (NanoSPR devices, USA), with a LED light source, λ = 650 nm, and a prism, refractive index *n* = 1.61, were used. The SPR measurements were performed using a home-built flow cell. Electropolymerization was performed using a Pt wire (diameter 0.5mm) counter electrode and a Ag wire quasi-reference electrode (diameter = 0.5 mm) which were installed in the cell (vol. 0.5 ml, working electrode area 0.2 cm<sup>2</sup>). Au-coated semi-transparent glass plates (Mivitec GmbH, Analytical μ-systems, Germany) were used as working electrodes. A PC-controlled (Autolab GPES software) electrochemical analyzer potentiostat/galvanostat (μAutolab, type III) was employed.

## Results and discussion

Au NPs, *ca.* 4.5 ± 0.5 nm, were functionalized with a capping monolayer consisting of 4-mercaptoaniline, (1), mercaptoethane sulfonic acid, (2), and mercaptophenyl boronic acid (3). The thioaniline units act as electropolymerizable components, the mercaptoethane sulfonate units enhance the stability of the NPs in aqueous media and prevent the precipitation of the NPs, and the mercaptophenyl boronic acid units provide the functional anchoring ligands for the covalent association of the saccharide molecules, Scheme 1. The modified Au NPs were electropolymerized on Au-coated glass surfaces in the absence (to fabricate the non-imprinted composite) or in the presence of the respective saccharide as imprint molecule, to yield the bis-aniline-crosslinked Au NP composite. The resulting polymer composites were rinsed with HEPES buffer 0.05 M, pH = 9.2, to remove the



**Scheme 1** Imprinting of saccharides (for example D-glucose) molecular recognition sites by electropolymerization of a bis-aniline-crosslinked Au NP composite on a Au surface.



**Scheme 2** Molecular structure of saccharides used in this study.

imprinted saccharides and to yield the respective imprinted or non-imprinted Au NP composites on the Au electrode surfaces. The monosaccharides, D-glucose, (4), L-glucose, (5), D-mannose, (6), D-galactose, (7), and the disaccharide, sucrose, (8), were used to yield the imprinted bis-aniline-crosslinked Au NP composites, Scheme 2. After removal of the imprinting mono- or disaccharide molecules from the Au NP composites, by treatment with an aqueous acidic solution, pH = 1.3, the imprinted (as well as the non-imprinted) matrices were equilibrated with an aqueous basic buffer solution, pH = 9.2, and subsequently challenged with the respective saccharides.

The Au NP matrices were prepared by the application of 10 electropolymerized cycles between  $-0.25$  V and  $0.7$  V vs. a Ag wire (QRE), followed by the application of 4 potential steps,  $E_{\text{final}} = 0.7$  V vs. Ag wire, 30 min each. The electropolymerization was followed by the *in situ* monitoring of the SPR curve shift of the surface. Coulometric analysis of the redox wave associated with the bis-aniline bridging units and complementary microgravimetric quartz-crystal-microbalance measurements indicated that the content of Au NPs in the electropolymerized matrices generated in the absence or in the presence of the imprint molecules was identical. The surface was characterized by AFM and exhibited an average thickness of ca. 11 nm. Knowing the dimensions of a single Au NP, this value translates to an average coverage of ca. 3 random densely packed layers of the Au NPs. The binding of the guest saccharide molecules to the imprinted or non-imprinted Au NP matrices was monitored by following the reflectance changes of the surface plasmon resonance spectra originating from the refractive-index changes of the composite as a result of the association of the saccharides to the Au NP matrices, and the consequent effect of the binding on the coupling between the localized plasmon of the Au NPs with the surface plasmon wave.

Fig. 1A shows the SPR curve fragment of the D-glucose-imprinted Au NPs composite before (curve a), and after (curve b) treatment of the matrix with  $100 \mu\text{M}$  D-glucose. A clear shift of the SPR spectrum is observed upon the binding of D-glucose to the Au NPs matrix. For comparison, the inset in Fig. 1A depicts

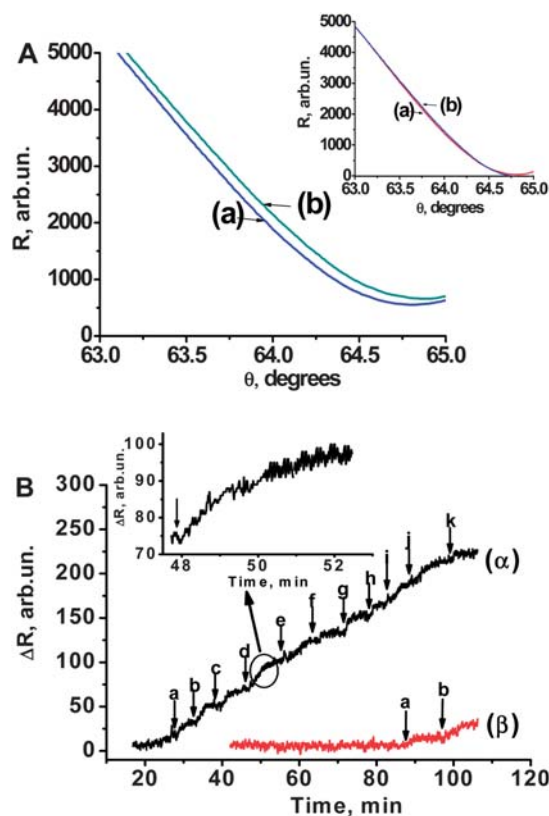


**Fig. 1** A, SPR curves corresponding to the D-glucose-imprinted and non-imprinted (inset) bis-aniline-crosslinked Au NP composite: (a) before the addition of D-glucose and (b) after the addition of D-glucose,  $100 \mu\text{M}$ . B, (a): Time-dependent reflectance changes (sensogram) of the imprinted surface upon the addition of variable concentrations of D-glucose: a, 40 pM, b, 200 pM, c, 1 nM, d, 4 nM, e, 20 nM, f, 100 nM, g, 200 nM, h, 1  $\mu\text{M}$ , i, 4  $\mu\text{M}$ , j, 20  $\mu\text{M}$ , k, 100  $\mu\text{M}$ . Inset: Enlarged time-dependent reflectance changes upon injection of 4 nM D-glucose. (b): Sensogram corresponding to the addition of (a) 100  $\mu\text{M}$ , (b) 200  $\mu\text{M}$  of D-glucose to the non-imprinted surface. Arrows indicate the time of addition of the analyte. All measurements were performed in a 50 mM HEPES buffer solution (pH = 9.2), at  $\theta = 63.5^\circ$ .

the SPR curve fragment at the same reflectance angle range for the non-imprinted matrix, before (curve a), and after (curve b) addition of  $100 \mu\text{M}$  D-glucose. A minute shift in the SPR curve is observed as a result of interaction of the non-imprinted Au NP composite with D-glucose. Fig. 1B, curves (a) and (b), depicts the sensograms, measured at a constant angle of  $\theta = 63.5^\circ$ , corresponding to the reflectance changes of the D-glucose-imprinted and non-imprinted Au NP composites-modified surfaces, respectively, upon interaction of the imprinted matrix with increasing concentrations of D-glucose. Fig. 1B, inset, shows a magnified region of the time-dependent reflectance changes upon interaction of the imprinted matrix with D-glucose, 4 nM. The reflectance changes level off to a constant value, after ca. 3 min, suggesting that this time-interval is required to equilibrate the analyte with the imprinted matrix, and it presents the response time of the sensor. The reflectance changes for the imprinted matrix are intensified as the concentration of D-glucose increases, and they level off at a micromolar concentration range. Clearly, the non-imprinted Au NPs matrix does not respond to added D-glucose, at this concentration range. The reflectance

changes observed with the imprinted matrix are significantly higher, indicating the enhanced binding of D-glucose to the imprinted matrix. This is attributed to the fact that the electropolymerization of the Au NPs, in the presence of D-glucose yielded molecularly imprinted sites with structural contours for D-glucose. The sites include the boronic acid ligands in positions inside the imprinted domains adopted for binding D-glucose (Scheme 1). The imprinting process is driven by interactions of boronic acid ligands and the vicinal diols of the monosaccharides that form cyclic boronate complexes with the phenyl boronic acid units associated with the Au NPs.

It should be noted that within the reported concentration range of D-glucose, changes in the refractive index of the solution, due to the addition of D-glucose, do not affect the SPR spectrum of the interface.

A set of further control experiments indicated the significance of the boronic acid ligands associated with the NPs in the selective and sensitive analysis of glucose. In one control experiment we electropolymerized on the Au surface thioaniline/mercaptoethane sulfonic acid-functionalized Au NPs that lacked the mercaptophenyl boronic acid ligand. The resulting composite did not show any reflectance changes upon interaction with D-glucose, implying that the association of the monosaccharide with the boronic acid ligand is essential to enable the analysis of D-glucose. In a further control experiment, mercaptophenyl boronic acid monolayer was assembled on the Au surface. The modified surface that lacked the Au NPs showed a reflectance change only at a concentration range starting at 0.5 mM. This concentration is *ca.* 10-fold higher than the concentration of D-glucose that gave a reflectance change with the non-imprinted Au NP composite and 10<sup>6</sup>-fold higher than the initial response concentration of the D-glucose-imprinted Au NPs composite. Clearly, the Au NPs amplify the SPR reflectance changes, as a result of the coupling between the localized plasmon of the NPs and the surface plasmon wave. Furthermore, the high signal in the presence of the imprinted composite reflects the high affinity of D-glucose to the imprinted sites.

The stereospecific binding affinity and selectivity of the D-glucose-imprinted Au NPs matrix to other monosaccharides was further investigated. Fig. 2A shows the reflectance changes of the D-glucose-imprinted composite upon interaction with D-glucose, sensogram ( $\alpha$ ), and upon interaction of the imprinted composite with variable concentrations of D-mannose, sensogram ( $\beta$ ), and of D-galactose, sensogram ( $\gamma$ ). Fig. 2B depicts the corresponding derived calibration curves. Measurable reflectance changes for the non-imprinted ("foreign") monosaccharides are observed only at high concentrations (in a micromolar range), and these level off to substantially lower saturation values. In control experiments, we find that reflectance changes for analyzing D-mannose and D-galactose by the non-imprinted Au NPs composite are observed only in the micromolar range and exhibit the same reflectance changes upon analysis of the monosaccharides. Thus, the results clearly indicate that D-mannose and D-galactose are discriminated by the D-glucose-imprinted composite, and the selective analysis of D-glucose is demonstrated. That is, although the three monosaccharides exhibit similar dimensions and carry a similar number of adjacent hydroxyl groups, an impressive selectivity for the detection of the imprinted monosaccharides is observed. The resulting selectivity

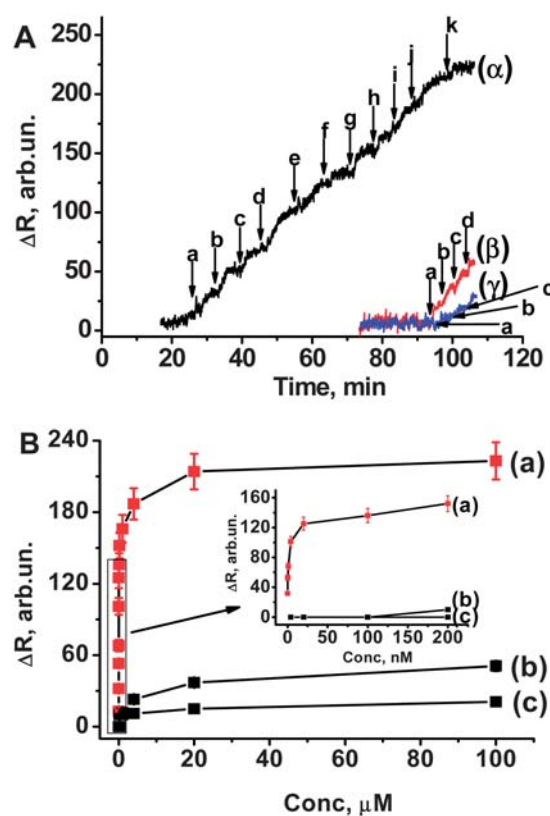
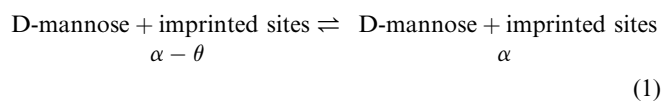


**Fig. 2** A, ( $\alpha$ ): Time-dependent reflectance changes (sensogram) of the D-glucose-imprinted surface upon addition of variable concentrations of D-glucose: a, 40 pM, b, 200 pM, c, 1 nM, d, 4 nM, e, 20 nM, f, 100 nM, g, 200 nM, h, 1  $\mu$ M, i, 4  $\mu$ M, j, 20  $\mu$ M, k, 100  $\mu$ M. ( $\beta$ ): Sensogram corresponding to the addition of: a, 4  $\mu$ M, b, 20  $\mu$ M, c, 100  $\mu$ M, d, 200  $\mu$ M of D-mannose to the D-glucose-imprinted surface. ( $\gamma$ ): Sensogram corresponding to the addition of: a, 20  $\mu$ M, b, 100  $\mu$ M, c, 200  $\mu$ M of D-galactose to the D-glucose-imprinted surface. B, Calibration curves corresponding to the reflectance changes of the D-glucose-imprinted Au NP composite at different concentrations of added: (a) D-glucose, (b) D-mannose and (c) D-galactose, to the imprinted surface. Inset: Lower concentrations region of the calibration curves.

is attributed to the imprinting procedure. The imprinted structural contours result in the steric orientation of the boronic acid ligands to hydroxyl functionalities of D-glucose in the appropriate configuration to yield the respective boronate esters. The boronic acid ligands in the D-glucose-imprinted Au NP composite are, however, sterically non-adapted to bind the isomeric OH-functionalities of D-mannose or D-galactose, leading to lower binding affinity of these molecules to the sites, and, eventually, to the weaker association of the "foreign" monosaccharides to "imperfect" imprinted sites. This leads to the observation of reflectance changes only at high bulk concentrations of the foreign monosaccharides, and to the formation of saturated reflectance changes with substantially lower reflectance-change values. It should be noted that the selectivity and the sensing features of the D-glucose-imprinted Au NPs composite are preserved after the sensing of the foreign monosaccharide. We find that the high value reflectance changes of the Au NPs are regenerated after completing one cycle of analyzing D-glucose, D-mannose, D-galactose and re-analyzing D-glucose (after analyzing each of the monosaccharides the Au NPs

composite was rinsed). In fact, the reflectance changes upon analyzing D-glucose in the second analysis cycle are slightly higher (ca. 15% higher) than the reflectance changes upon analyzing D-glucose in the first cycle. This is attributed to the removal of residual trace amounts of D-glucose from the Au NPs composite upon analyzing the D-mannose and D-galactose and the application of the respective rinsing steps. That is, since the imprinting procedure involves a high concentration of the imprinting template (0.5 M), the rinsing of the matrix (under acidic conditions) leaves residues of specifically and non-specifically bound monosaccharide molecules in the composite. In subsequent sensing cycles, the matrices are treated with low concentrations of the analytes, thus allowing the complete removal of the bound saccharides. It should be noted that the sensing interface could be regenerated by rinsing of the bound monosaccharide for at least a further five sensing cycles with signal reproducibility of  $\pm 5\%$ .

To demonstrate the generality of the imprinting process toward the development of specific Au NP matrices for the detection of monosaccharides, we imprinted D-mannose or D-galactose in the Au NP composites by the analogous electro-polymerization of the boronic acid-functionalized Au NPs on the thioaniline modified electrode, in the presence of the respective monosaccharide. Fig. 3A shows the reflectance changes of the D-mannose-imprinted composite, upon interaction with variable concentrations of D-mannose, sensogram ( $\alpha$ ). The reflectance changes increase as the concentration of D-mannose in the buffer solution is elevated, and they level off at ca. 20 nM, implying that all the imprinted sites are saturated with D-mannose. For comparison, the sensograms of the imprinted matrix upon interaction with D-galactose, sensogram ( $\beta$ ), and D-glucose, sensogram ( $\gamma$ ), are presented. Fig. 3B depicts the derived calibration curves in the same concentration range. Clearly, D-mannose-imprinted matrix reveals a high affinity for the binding of the imprinted substrate, D-mannose, detection limit 40 pM, while exhibiting substantially lower binding affinities for the “foreign” monosaccharides, D-galactose and D-glucose, respectively, (detection limits of 20  $\mu$ M and 40  $\mu$ M, respectively). For comparison, Fig. 3B, curve (d) shows the calibration curve corresponding to the reflectance changes of the non-imprinted Au NP composite upon interaction with variable concentrations of D-mannose. Clearly, the affinity of the non-imprinted matrix for the detection of D-mannose in this concentration range is very low. This re-emphasizes the importance of the imprinting process in generating a highly sensitive and selective sensing composite. The association of D-mannose to the imprinted sites follows a Langmuir-type binding, eqn (1), from which the association constant of D-mannose to the imprinted sites,  $K_{\text{ass}}$ , eqn (2), was estimated to be  $K_{\text{ass}} = 4 \times 10^9 \text{ M}^{-1}$ ,



$$K_{\text{ass}} = \frac{\theta}{(\alpha - \theta)[\text{D-mannose}]} \quad (2)$$

where  $\theta$  is the number of sites occupied by D-mannose and  $\alpha$  is the total number of binding sites.

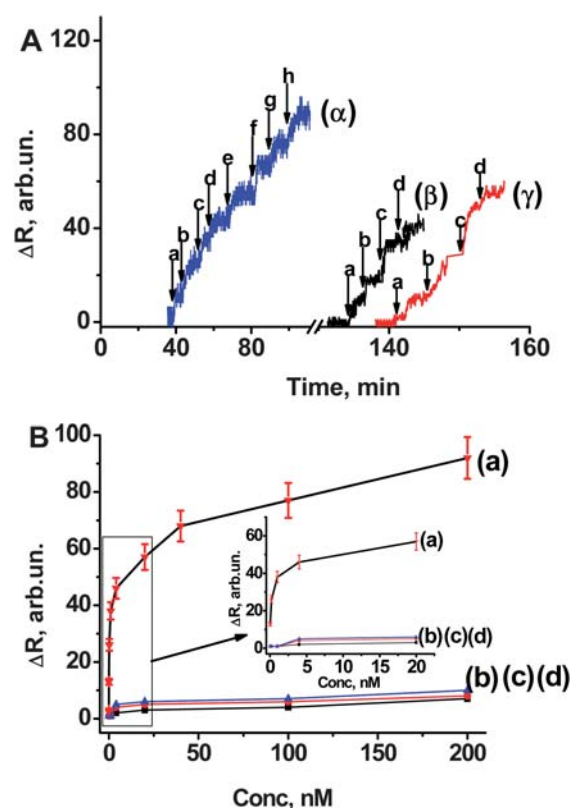


**Fig. 3** A, ( $\alpha$ ): Time-dependent reflectance changes (sensogram) of the D-mannose-imprinted Au NP-modified surface upon the addition of variable concentrations of D-mannose: a, 40 pM, b, 200 pM, c, 1 nM, d, 4 nM, e, 20 nM, f, 40 nM, g, 100 nM, h, 200 nM. ( $\beta$ ): Sensogram corresponding to the addition of: a, 20  $\mu$ M, b, 100  $\mu$ M, c, 200  $\mu$ M, d, 1 mM of D-galactose to the D-mannose-imprinted surface. ( $\gamma$ ): Sensogram corresponding to the addition of: a, 20  $\mu$ M, b, 100  $\mu$ M, c, 200  $\mu$ M, d, 1 mM of D-glucose to the D-mannose-imprinted surface. B, Calibration curves corresponding to the reflectance changes of the D-mannose-imprinted NP composite, upon the addition of variable concentrations of: (a) D-mannose, (b) D-galactose and (c) D-glucose to the imprinted surface. (d): Reflectance changes upon addition of different concentrations of D-mannose to the non-imprinted bis-aniline-crosslinked surface. Inset: Lower concentrations region of the calibration curves.

Similarly, D-galactose was analyzed by the D-galactose-imprinted Au NPs composite, and the selectivity of the imprinted matrix was examined. Fig. 4A, sensogram ( $\alpha$ ) shows the reflectance changes of the D-galactose-imprinted Au NP composite upon treatment with variable concentrations of D-galactose. The reflectance changes increase upon elevating the concentrations of D-galactose in the buffer solution, Fig. 4A, and they level off at a concentration corresponding to ca. 50 nM, implying that all the imprinted sites are saturated with D-galactose. The resulting D-galactose-imprinted matrix revealed the effective sensing of the imprinted substrate. The corresponding calibration curve is depicted in Fig. 4B, (a), implying that D-galactose could be detected with a detection limit of ca. 10 pM. The D-galactose-imprinted Au NPs revealed similar selectivity, and only minute reflectance changes could be observed upon interaction of the D-galactose-imprinted Au NPs composite with D-glucose or D-mannose at a micromolar range, see Fig. 4A, sensograms  $\beta$  and  $\gamma$ , respectively, and Fig. 4B, curves (b) and (c), respectively. The

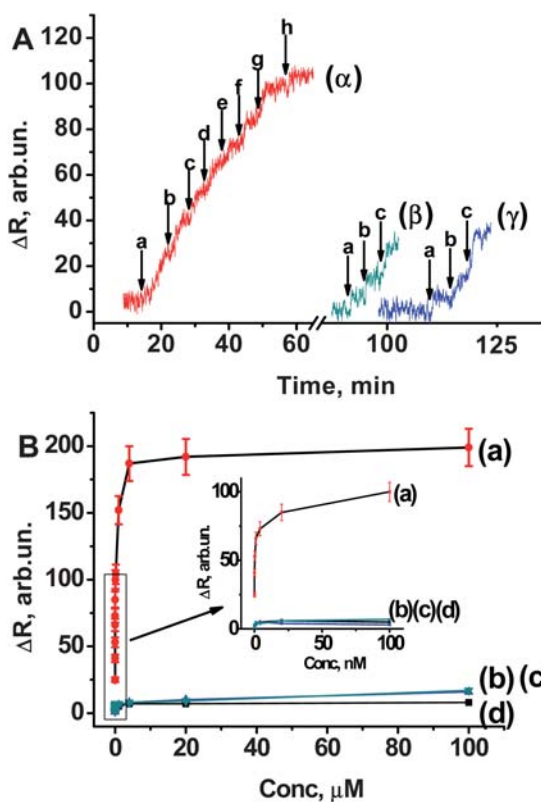


**Fig. 4** A, (α): Time-dependent reflectance changes (sensogram) of the D-galactose-imprinted Au NP-modified surface upon addition of variable concentrations of D-galactose: a, 10 pM, b, 40 pM, c, 200 pM, d, 1 nM, e, 4 nM, f, 20 nM, g, 100 nM, h, 200 nM. (β): Sensogram corresponding to the addition of: a, 20 μM, b, 100 μM, c, 200 μM of D-glucose to the D-galactose-imprinted surface. (γ): Sensogram corresponding to the addition of: a, 20 μM, b, 100 μM, c, 200 μM of D-mannose to D-galactose-imprinted surface. B, Calibration curves corresponding to the reflectance changes of the D-galactose-imprinted Au NP matrix at different concentrations of: (a) D-galactose, (b) D-glucose and (c) D-mannose to the imprinted surface. (d): The reflectance changes upon addition of different concentrations of D-galactose to the non-imprinted bis-aniline-cross-linked Au NPs-modified surface. Inset: Lower concentrations region of the calibration curves.

association constant of D-galactose to the D-galactose-imprinted sites was estimated to be  $1.1 \times 10^{10} \text{ M}^{-1}$ . Also, the non-imprinted Au NPs composite revealed low affinity for the association of D-galactose. Only minute reflectance changes  $\Delta R = 9 \pm 3$  at the concentrations lower than 100 μM of the substrate were observed, Fig. 4B, curve (d).

As the results indicate that imprinting of the monosaccharides into Au NP composites leads to impressive stereoselectivity, we examined the possibility of yielding chiroselective Au NP matrices by the application of the imprinting process. Towards this goal, we applied the D-glucose-imprinted Au NP composite to the analysis of L-glucose. Fig. 5A, sensograms (α) and (β), shows the reflectance changes of the D-glucose-imprinted Au NP composite upon interaction with D-glucose and L-glucose, respectively. Evidently, the reflectance changes are substantially higher upon interaction with D-glucose, and the reflectance changes are observed at a substantially lower concentration corresponding to a detection limit of 10 pM. The respective

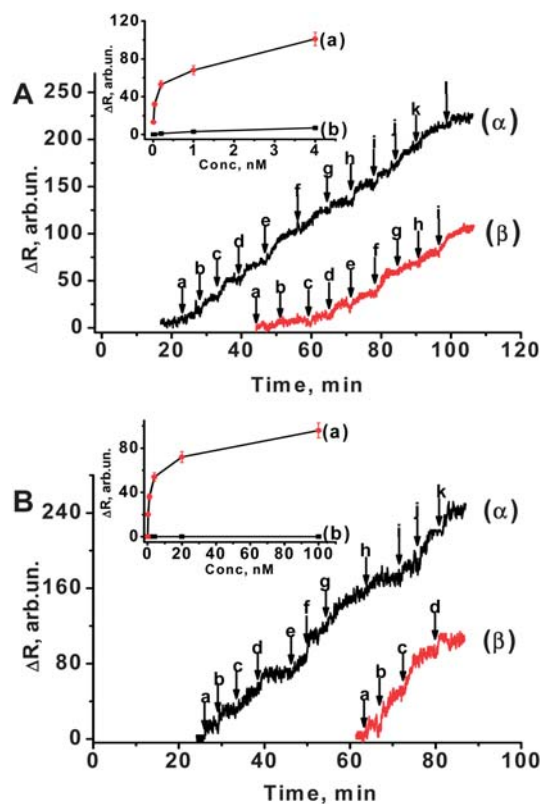


**Fig. 5** A, (α) Time-dependent reflectance changes (sensogram) of D-glucose-imprinted surface upon addition of variable concentrations of D-glucose: a, 10 pM, b, 40 pM, c, 200 pM, d, 1 nM, e, 4 nM, f, 20 nM, g, 100 nM, h, 200 nM, i, 1 μM, j, 4 μM, k, 20 μM, l, 100 μM. (β): Sensogram corresponding to the addition of: a, 1 nM, b, 4 nM, c, 20 nM, d, 100 nM, e, 200 nM, f, 1 μM, g, 4 μM, h, 20 μM, i, 100 μM, of L-glucose to the D-glucose-imprinted surface. Inset: Calibration curves corresponding to the reflectance changes at different concentrations of added: (a) D-glucose and (b) L-glucose to the D-glucose-imprinted surface. B, (α) Time-dependent reflectance changes (sensogram) of the L-glucose-imprinted surface upon addition of variable concentrations of L-glucose: a, 200 pM, b, 1 nM, c, 4 nM, d, 20 nM, e, 100 nM, f, 200 nM, g, 1 μM, h, 4 μM, i, 20 μM, j, 100 μM, k, 200 μM. (β): Sensogram corresponding to the addition of: a, 4 μM, b, 20 μM, c, 100 μM, d, 200 μM of D-glucose to the L-glucose-imprinted surface. Inset: Calibration curves corresponding to the reflectance changes at variable concentrations of added: (a) L-glucose and (b) D-glucose to the L-glucose-imprinted surface.

calibration curves are depicted in Fig. 5A, inset. These results are consistent with the fact that the D-glucose-imprinted sites reveal improved steric fit for the binding of D-glucose over the association of L-glucose to the imprinted sites. The results are reversed upon the imprinting of L-glucose sites in the Au NPs composite. Fig. 5B, sensograms (α) and (β), shows the reflectance changes upon interaction of the L-glucose-imprinted composite with L-glucose and D-glucose, respectively. Fig. 5B, inset, depicts the resulting calibration curves. Evidently, the L-glucose-imprinted Au NPs matrix reveals enhanced affinity for the association of L-glucose, as compared to the binding of D-glucose. From the respective calibration curves, we estimate the association constants of D-glucose and L-glucose, to the D-glucose-imprinted sites to be  $K_a^{DP} = 8.3 \times 10^9 \text{ M}^{-1}$  and  $K_a^{LP} = 4.4 \times 10^6 \text{ M}^{-1}$ , and of the L-glucose and D-glucose to the L-glucose-imprinted sites to

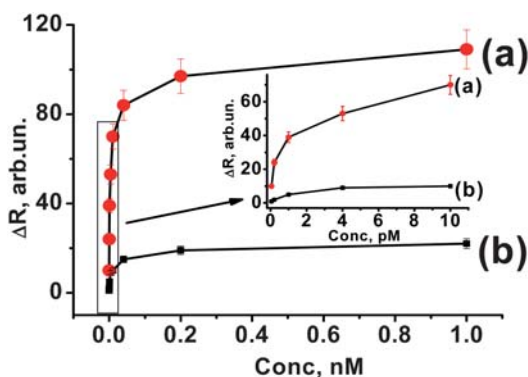


**Fig. 6** Calibration curves corresponding to the reflectance changes upon the interaction of the sucrose-imprinted Au NP composite with variable concentrations of: (a) sucrose and (b) D-glucose. Inset: Lower concentrations region of the calibration curves.

be  $K_a^{LL} = 1.2 \times 10^9 \text{ M}^{-1}$  and  $K_a^{DL} = 1.3 \times 10^5 \text{ M}^{-1}$ , respectively. We thus conclude that chiroselective, imprinted recognition sites may be generated in the electropolymerized Au NP composites.

Control experiments revealed, as expected, that the non-imprinted Au NPs composite showed minute and similar reflectance changes upon interaction with D-glucose and L-glucose, respectively. Realizing that the imprint of the monosaccharide recognition sites originates from the formation of boronate complexes with the vicinal hydroxyl functionalities associated with the monosaccharides, one may envisage that improved recognition sites would be generated upon imprinting disaccharides, or even higher oligomers, due to the increased number of boronic acid ligation sites. Accordingly, we implemented sucrose as the imprint molecule. As sucrose consists of D-glucose and fructose units linked by a glycoside bond, one could examine the selectivity of the sucrose-imprinted site towards the D-glucose. Fig. 6, curve (a), depicts the calibration curve for the analysis of different concentrations of sucrose by the sucrose-imprinted Au NP composite. The disaccharide is sensed with an impressive sensitivity of ca. 200 fM, consistent with the formation of a high-affinity imprinted binding site for the disaccharide,  $K_{\text{ass}}^{\text{sucrose}} = 2.5 \times 10^{12} \text{ M}^{-1}$ . As before, the reflectance changes of the non-imprinted Au NPs composite upon interaction with sucrose were found to be very low, and detectable only at higher concentrations of the disaccharide. As expected, the D-glucose-imprinted Au NPs composite shows only minute reflectance changes upon interaction with sucrose. This result is reasonable, due to the larger size of sucrose (as compared with D-glucose) that cannot be accommodated in the small-sized D-glucose-imprinted sites. The possible binding of D-glucose to the sucrose-imprinted sites should be, however, addressed (specifically since D-glucose is a subunit of sucrose). Fig. 6, curve (b) shows the reflectance changes of the sucrose-imprinted Au NPs composite upon interaction with different concentrations of D-glucose. The reflectance changes are observed at higher concentrations of D-glucose, revealing substantially lower reflectance changes. These results suggest that although D-glucose is a subunit of sucrose, its affinity to the sucrose-imprinted sites is substantially weaker. That is, although the sucrose-imprinted sites have the dimensions to accommodate D-glucose, the binding of the monosaccharide to the sucrose-imprinted sites is substantially lower than that of

sucrose. This is due to the fact that the association of sucrose is synergetically stabilized by several boronic acid ligands. From these calibration curves we estimate the binding constants of sucrose and D-glucose to the sucrose-imprinted sites to be  $K_1 = 2.5 \times 10^{12} \text{ M}^{-1}$  and  $K_2 = 1 \times 10^7 \text{ M}^{-1}$ , respectively.

## Conclusions

This study highlights a sensitive label-free sensing platform for the stereoselective and chiroselective analysis of monosaccharides and disaccharides. Imprinting of the molecular recognition sites is based on the use of thioaniline/mercaptophenyl boronic acid as a functional capping layer of the Au NPs. Electropolymerization of the NPs in the presence of the saccharide bound to the boronic acid ligands leads to the formation of bis-aniline-bridged Au NP composites that, after removal of the respective saccharide, yield the imprinted matrices. Binding of the saccharides to the sensing matrices is followed by SPR spectroscopy. Dielectric changes upon binding of the saccharides to the sensing matrices result in a shift of the SPR spectra. In particular, coupling between the localized plasmon of the Au NPs and the surface plasmon wave amplifies the SPR curve shifts, caused by the dielectric changes occurring upon binding of the saccharides to the NP matrices. This enables the sensitive stereoselective and chiroselective detection of the different saccharides.

## Acknowledgements

This study is supported by the Converging Technologies Program, the Israel Science Foundation. M.R. is supported by the CAMBR fellowship.

## References

- (a) K. Haupt, *Analyst*, 2001, **126**, 747–756; (b) B. Sellergren, *TrAC, Trends Anal. Chem.*, 1997, **16**, 310–320; (c) F. Lanza and B. Sellergren, *Anal. Chem.*, 1999, **71**, 2092–2096; (d) M. J. Whitcombe and E. N. Vulfsen, *Adv. Mater.*, 2001, **13**, 467–478; (e) K. Haupt and K. Mosbach, *Chem. Rev.*, 2000, **100**, 2495–2504.
- (a) G. Wulff, *Angew. Chem., Int. Ed. Engl.*, 1995, **34**, 1812–1832; (b) O. Brüggemann, K. Haupt, L. Ye, E. Yilmaz and K. Mosbach, *J. Chromatogr., A*, 2000, **889**, 15–24; (c) A. Katz and M. E. Davis, *Nature*, 2000, **403**, 286–289; (d) M. Glad, D. Norrlov, B. Sellergren, N. Siegbahn and K. J. Mosbach, *J. Chromatogr., A*, 1985, **347**, 11–15; (e) T. L. Panasyuk, V. M. Mirsky, S. A. Piletsky and O. S. Wolfbeis, *Anal. Chem.*, 1999, **71**, 4609–4613.
- (a) J. M. Lin, T. Nakagama, K. Uchiyama and T. Hobo, *Chromatographia*, 1996, **43**, 585–591; (b) L. Schweitz, P. Spéjel and S. Nilsson, *Analyst*, 2000, **125**, 1899–1901; (c) O. Brüggemann, K. Haupt, L. Ye, E. Yilmaz and K. Mosbach, *J. Chromatogr., A*, 2000, **889**, 15–24.
- (a) M. Li, S. Tang, F. Shen, M. Liu, W. Xie, H. Xia, L. Liu, L. Tian, Z. Xie, P. Lu, M. Hanif, D. Lu, G. Cheng and Y. Ma, *Chem. Commun.*, 2006, 3393–3395; (b) K. M. Maness, R. H. Terrill, T. J. Meyer, R. W. Murray and R. M. Wightman, *J. Am. Chem. Soc.*, 1996, **118**, 10609–10616; (c) S. Komaba, A. Amano and T. Osaka, *J. Electroanal. Chem.*, 1997, **430**, 97–102.
- (a) K. Morihara, M. Kurokawa, Y. Kamata and T. Shimada, *J. Chem. Soc., Chem. Commun.*, 1992, 358–360; (b) J. V. Beach and K. J. Shea, *J. Am. Chem. Soc.*, 1994, **116**, 379–380; (c) J. Matsui, I. A. Nicholls, I. Karube and K. J. Mosbach, *J. Org. Chem.*, 1996, **61**, 5414–5417.

- 6 (a) F. L. Dickert and M. Tortschanoff, *Anal. Chem.*, 1999, **71**, 4559–4563; (b) T. L. Panasyuk, V. M. Mirsky, S. A. Piletsky and O. S. Wolfbeis, *Anal. Chem.*, 1999, **71**, 4609–4613.
- 7 E. Granot, R. Tel-Vered, O. Lioubashevski and I. Willner, *Adv. Funct. Mater.*, 2008, **18**, 478–484.
- 8 (a) M. Lahav, A. B. Kharitonov, O. Katz, T. Kunitake and I. Willner, *Anal. Chem.*, 2001, **73**, 720–723; (b) M. Zayats, M. Lahav, A. B. Kharitonov and I. Willner, *Tetrahedron*, 2002, **58**, 815–824.
- 9 S. W. Lee, I. Ichinose and T. Kunitake, *Langmuir*, 1998, **14**, 2857–2863.
- 10 W. Wang, S. Gao and B. Wang, *Org. Lett.*, 1999, **1**, 1209–1212.
- 11 (a) J. Matsui, I. A. Nicholls and T. Takeuchi, *Tetrahedron: Asymmetry*, 1996, **7**, 1357–1361; (b) O. Ramstrom, I. A. Nicholls and K. Mosbach, *Tetrahedron: Asymmetry*, 1994, **5**, 649–656; (c) P. T. Vallano and V. T. Remcho, *J. Chromatogr., A*, 2000, **887**, 125–135.
- 12 M. Lahav, A. B. Kharitonov and I. Willner, *Chem. Eur. J.*, 2001, **7**, 3992–3997.
- 13 (a) G. Schmid, *Chem. Rev.*, 1992, **92**, 1709–1727; (b) M. M. Alvarez, J. T. Houry, T. G. Schaaff, M. N. Shafiqullin, I. Vezmar and R. L. Whetten, *J. Phys. Chem. B.*, 1997, **101**, 3706–3712.
- 14 M. Zayats, R. Baron, I. Popov and I. Willner, *Nano Lett.*, 2005, **5**, 21–25.
- 15 (a) L. E. Brus, *Appl. Phys. A: Mater. Sci. Process*, 1991, **53**, 465–474; (b) U. Nickel, P. Halbig, H. Gliemann and S. Schneider, *Ber. Bunsenges. Phys. Chem.*, 1997, **101**, 41–49.
- 16 (a) J. J. Storhoff and C. A. Mirkin, *Chem. Rev.*, 1999, **99**, 1849–1862; (b) M. C. Daniel and D. Astruc, *Chem. Rev.*, 2004, **104**, 293–346.
- 17 (a) R. C. Mucic, J. J. Storhoff, C. A. Mirkin and R. L. Letsinger, *J. Am. Chem. Soc.*, 1998, **120**, 12674–12675; (b) J. Liu and Y. Lu, *J. Am. Chem. Soc.*, 2003, **125**, 6642–6643; (c) J. Liu and Y. Lu, *Anal. Chem.*, 2004, **76**, 1627–1632.
- 18 (a) E. Katz, I. Willner and J. Wang, *Electroanalysis*, 2004, **16**, 19–44; (b) A. N. Shipway, M. Lahav, R. Blonder and I. Willner, *Chem. Mater.*, 1999, **11**, 13–15; (c) J. Wang, G. Liu and J. Merkoci, *J. Am. Chem. Soc.*, 2003, **125**, 3214–3215.
- 19 (a) H. Raether, in *Surface Plasmons on Smooth and Rough Surfaces and on Gratings*, Springer Tracts in Modern Physics, Springer-Verlag, New-York, 1988, vol. 111; (b) W. Knoll, *Annu. Rev. Phys. Chem.*, 1998, **49**, 569–638; (c) A. Bada, R. C. Advincula and W. Knoll, in *Novel Methods To Study Interfacial Layers*, ed. D. Mobius, R. Miller, *Studies in Interface Science*, Elsevier Science, New York, 2001, vol. 11, p 55.
- 20 (a) J. Homola, *Chem. Rev.*, 2008, **108**, 462–493; (b) K. S. Phillips and Q. Cheng, *Anal. Bioanal. Chem.*, 2007, **387**, 1831–1840; (c) S. Heyse, O. P. Ernst, Z. Dienes, K. P. Hofmann and H. Vogel, *Biochemistry*, 1998, **37**, 507–522; (d) C. E. H. Berger, T. A. M. Beumer, R. P. H. Kooyman and J. Greve, *Anal. Chem.*, 1998, **70**, 703–706; (e) M. Fivash, E. M. Towler and R. J. Fisher, *Curr. Opin. Biotechnol.*, 1998, **9**, 97–101.
- 21 S. Kubitschko, J. Spinke, T. Bruckner, S. Pohl and N. Oranth, *Anal. Biochem.*, 1997, **253**, 112–122.
- 22 T. Wink, S. J. van Zuilen, A. Bult and W. P. van Bennekom, *Anal. Chem.*, 1998, **70**, 827–832.
- 23 M. Zayats, O. A. Raitman, V. I. Chegel, A. B. Kharitonov and I. Willner, *Anal. Chem.*, 2002, **74**, 4763–4773.
- 24 (a) L. A. Lyon, M. D. Musick, P. C. Smith, B. D. Reiss, D. J. Pena and M. J. Natan, *Sens. Actuators, B*, 1999, **54**, 118–124; (b) G. S. Agarwal and S. Dutta Gupta, *Phys. Rev. B: Condens. Matter.*, 1985, **32**, 3607–3611; (c) W. R. Holland and D. G. Hall, *Phys. Rev. B: Condens. Matter.*, 1983, **27**, 7765–7768.
- 25 (a) L. A. Lyon, M. D. Musick and M. J. Natan, *Anal. Chem.*, 1998, **70**, 5177–5183; (b) E. Mauriz, A. Calle, L. M. Lechuga, J. Quintana, A. Montoya and J. Manclus, *Anal. Chim. Acta*, 2006, **561**, 40–47.
- 26 L. He, M. D. Musick, S. R. Nicewarner, F. G. Sallinas, S. J. Benkovic, M. J. Natan and C. D. Keating, *J. Am. Chem. Soc.*, 2000, **122**, 9071–9077.
- 27 M. Zayats, S. P. Pogorelova, A. B. Kharitonov, O. Lioubashevski, E. Katz and I. Willner, *Chem. Eur. J.*, 2003, **9**, 6108–6114.
- 28 M. Riskin, R. Tel-Vered, T. Bourenko, E. Granot and I. Willner, *J. Am. Chem. Soc.*, 2008, **130**, 9726–9733.
- 29 M. Riskin, R. Tel-Vered, O. Lioubashevski and I. Willner, *J. Am. Chem. Soc.*, 2009, **131**, 7368–7378.
- 30 M. Riskin, R. Tel-Vered and I. Willner, *Adv. Mater.*, 2010, **22**, 1387–1391.
- 31 M. Riskin, R. Tel-Vered, M. Frasconi, N. Yavo and I. Willner, *Chem. Eur. J.*, 2010, **16**, 7114–7120.
- 32 (a) T. D. James, in *Boronic Acids: Preparation and Applications in Organic Synthesis and Medicine*, ed. D. G. Hall, Wiley-VCH, Weinheim, 2005, pp. 441–479; (b) J. Lorand and J. O. Edwards, *J. Org. Chem.*, 1959, **24**, 769–774; (c) T. D. James and S. Shinkai, *Top. Curr. Chem.*, 2002, **218**, 159–200; (d) A. P. de Silva, H. Q. N. Gunaratne, A. J. M. Huxley, C. P. McCoy, J. T. Rademacher and T. E. Rice, *Chem. Rev.*, 1997, **97**, 1515–1566; (e) H. Eggert, J. Fredericksen, C. Morin and J. C. Norrild, *J. Org. Chem.*, 1999, **64**, 3846–3852.
- 33 (a) W. Wang, X. Gao and B. Wang, *Curr. Org. Chem.*, 2002, **6**, 1285–1317; (b) T. D. James, K. R. A. S. Sandanayake and S. Shinkai, *Angew. Chem., Int. Ed. Engl.*, 1996, **35**, 1910–1922; (c) D. B. Cordes, S. Gamsey and B. Singaram, *Angew. Chem., Int. Ed.*, 2006, **45**, 3829–3832; (d) S. M. Strawbridge, S. J. Green and J. H. R. Tucker, *Chem. Commun.*, 2000, 2393–2394; (e) H. B. Yildiz, R. Freeman, R. Gill and I. Willner, *Anal. Chem.*, 2008, **80**, 2811–2816.
- 34 R. Freeman, J. Elbaz, R. Gill, M. Zayats and I. Willner, *Chem. Eur. J.*, 2007, **13**, 7288–7293.
- 35 (a) G. Wulff and J. Gimpel, *Makromol. Chem.*, 1982, **183**, 2469–2477; (b) G. Wulff and S. Schauhoff, *J. Org. Chem.*, 1991, **56**, 395–400; (c) G. Wulff, H. Schmidt, H. Witt and R. Zentel, *Angew. Chem., Int. Ed. Engl.*, 1994, **33**, 188–191.
- 36 M. Frasconi, R. Tel-Vered, M. Riskin and I. Willner, *Anal. Chem.*, 2010, **82**, 2512–2519.